Advances in Chemical Engineering and Science, 2015, 5, 225-238
Published Online July 2015 in SciRes. http://www.scirp.org/journal/aces
http://dx.doi.org/10.4236/aces.2015.53024

Gas-Solid Flow Behavior in a Pneumatic Conveying System for Drying Applications: Coarse Particles Feeding with a Venturi Device

Thiago Faggion de Pádua, Rodrigo Béttega, José Teixeira Freire

Department of Chemical Engineering, Federal University of São Carlos, São Carlos, Brazil
Email: tfpadua@gmail.com

Received 12 May 2015; accepted 15 June 2015; published 19 June 2015

Abstract

The feeding of coarse particles (>0.5 mm diameter) directly into a riser operating at positive pressure is important for drying and pre-heating applications. The presence of the feeding device can lead to heterogeneity of drying and heating, and is the main factor responsible for pressure loss in short conveying systems. However, there is a lack of information concerning the axial and radial distributions of coarse particles in this type of configuration, despite the recent advances when dealing with fine particles (FCC catalyst). The present work therefore investigates a vertical venturi feeder with the conveying system operating in dilute-phase regime with 1 mm spherical glass particles. Experimental assays revealed the behavior of the mass flow rate of solids in the system, and pressure measurements were made along the riser in order to evaluate the accuracy of simulations. Euler-Euler simulations provided close estimation of the experimental pressure drop and the pressure drop according to distance in the linear region. Simulation of the fluid dynamics in the riser showed that solids clusters were formed at low concentrations near the feeding device, reflecting heterogeneity in the solid phase volume fraction.

Keywords

Pneumatic Conveying, Venturi Feeder, Coarse Particles, Drying, CFD

1. Introduction

Pneumatic conveying offers an alternative for the drying and pre-heating of solids [1]-[4]. One of its advantages

How to cite this paper: de Pádua, T.F., Béttega, R. and Freire, J.T. (2015) Gas-Solid Flow Behavior in a Pneumatic Conveying System for Drying Applications: Coarse Particles Feeding with a Venturi Device. *Advances in Chemical Engineering and Science*, **5**, 225-238. http://dx.doi.org/10.4236/aces.2015.53024

is that products or raw materials dry as they are being conveyed, and potential applications include the drying of cereals and pharmaceuticals, for example.

Various different dryer configurations have been proposed based on this concept, including the drying of paste materials by coating onto inert solids [4]. As for many other materials of interest, these inert solids are usually larger than 0.5 mm. Such applications have stimulated interest in conveying coarse particles through risers. Nevertheless, there have been few studies concerning the distributions of coarse particles in gas-solid flows in riser configurations intended for drying.

The majority of studies addressing coarse particles do not focus on drying. In this case, conveying typically occurs essentially in the horizontal direction, and the feeding section of the conveyor is oriented horizontally. Knowledge concerning the distribution of solids during horizontal pneumatic conveying has been summarized by Fokeer *et al*. [5]. In the case of risers, the entrance of the riser section is usually an elbow. Since bends are frequently employed to change the direction of solids being conveyed, there have been several simulation and experimental studies of particle rope formation in risers due to bends, and subsequent dissipation of these effects [6] [7].

As an alternative, solid feeding in the vertical orientation (directly into the riser) is an interesting configuration that can be used when the conveying occurs mainly in a riser [4] [8] [9].

Lopes *et al*. [9] used a venturi feeder with low positive pressure systems in vertical orientation, which could be used to feed powder or granular material into a riser for drying purposes. The feeding of material directly into the riser can decrease pressure drop, pipe wear, and particle degradation, since fewer bends are required in the system.

Other important issues can arise in relation to the mixing of solids and the homogeneity of drying in risers with vertical feeding. Moreover, much of the interphase momentum, heat and mass transfer take place in the acceleration region, where the slip velocity is high [10]. Therefore, it is important to understand the fluid dynamics near the solids feeding device, in applications such as the drying of solids. However, there is a paucity of information and experimental data concerning details of the two-phase flow near the feeding device and in the next region. CFD simulations can contribute to elucidation of this issue.

On the other hand, a lot of information has been collected in recent decades relating to the radial and axial distribution of fine particles (particularly FCC catalysts) in risers under distinct fluidization regimes and equipment configurations, motivated by conventional circulating fluidized bed (CFB) applications [11]-[13]. Unfortunately, it is not possible to generalize knowledge about gas-solid flows in risers for conventional CFB applications in order to understand drying equipment configurations and conditions. This is mainly due to the theoretical complexity of the mechanisms involved in conveying.

This paper investigates a riser with a venturi feeder in vertical orientation, operated with coarse particles (1 mm). The system was studied experimentally and by means of Eulerian CFD simulations. The feeder was similar to the one described by Lopes *et al*. [9]. The main goal was to analyze the solid phase distribution in the system, evaluating homogeneity and feeding device effects along the riser. Experimental data are presented, and the behavior of the solids mass flow according to the air flow rate in the system was revealed. Data emphasize the importance of scale-up for industrial application. Simulations of the gas-solid flow in this system were developed, and pressure measurements along the riser were used to verify numerical results. The simulated fluid dynamics of the multiphase flow in the system is analyzed and discussed. The solid mixing is the main concern and the present work contributes to providing information about the feeding of coarse particles directly into a riser with a venturi device, which is an important configuration for drying and pre-heating applications.

2. Materials and Methods

2.1. Experimental Materials and Methods

The conveyor (**Figure 1**) was constructed using galvanized iron pipe with internal diameter of 53.2 mm. The equipment consisted of the air feeding riser section (1 in **Figure 1**), the solids feeding device section (shaded part in **Figure 1**), a riser, a loop, and a downer.

A set of experiments were conducted to measure pressures at the wall along the conveyor, as well as the solids and gas flow rates.

The conveying air was provided by a 7.5 hp blower (Erberle, São Paulo, Brazil) and the air flow rate was measured using a previously calibrated venturi meter (2). The air flow rate was set by two globe valves (not

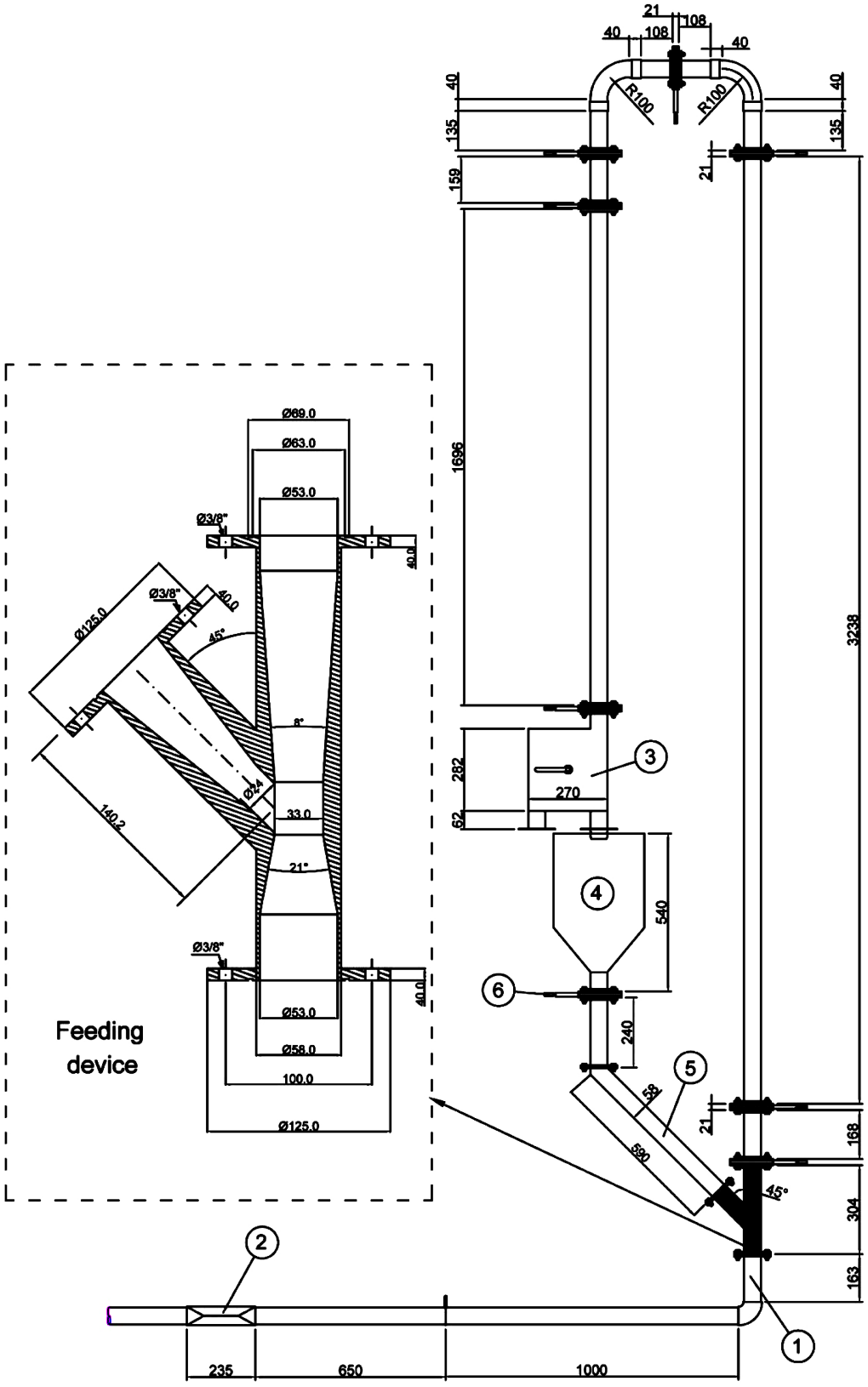

Figure 1. Pneumatic conveyor and venturi feeder (in mm). (1) Air entrance to the riser, (2) air flow meter, (3) solids sampler, (4) solids reservoir, (5) solids feeding pipe, (6) slide valve for solids discharge.

shown in **Figure 1**), one (bypass) used to divert the air and the other to restrict the passage of air in the horizontal pipe.

An amount of solids could be collected from the sampler connected after the downer (3) for a specified time, and the solid mass flow rate could be calculated. A description of the sampler can be found in Costa *et al*. [14].

The solids reservoir (4) followed the sampler and had a conical base with a cone angle of 60˚. The solids were discharged at the feeding device from a central orifice in the conical base, through an inclined (45˚) pipe (5) with internal diameter of 53.2 mm (here referred to as the solids feeding pipe). A slide valve located at the exit of the reservoir (6) could be used to set the discharge flow rate of solids by restricting the discharge area. The downward flow of material into the feeder was due only to gravity, and a custom-made venturi device was used in order to avoid adverse air leakage, which occurs through the feeding pipe in positive conveying systems [15].

The venturi feeder employed is shown in **Figure 1** (feeding device). This type of venturi feeder is designed to operate at low pressures due to the need to impose high constriction on the solids entrance area at higher pressures. Low-pressure systems operate under about 1 bar (gauge), as defined by Mills [15]. The feeding device differed from that described by Lopes *et al*. [9] due to the solids feeding pipe configuration, since there was no bend before the connection to the venturi throat.

Pressure transducers were connected to ten taps (**Table 1**) distributed along the riser and the feeding device. The t1 tap was located at the venturi feeder (**Figure 1**), before the nozzle at 21 mm following the entrance of the conveying air.

Data were collected with and without feeding of particles (using air alone and two-phase flow). The particles were spherical and made of glass with 1 mm diameter (ρ_s = 2512 kg/m^3).

The experimental procedure for the assays with solids feeding involved setting the air flow rate and initiating solids feeding at the specified discharge area restriction. Pressure data were acquired and recorded once steady state conveying was established. The procedure was repeated for all the air flow rates. **Table 2** lists the experimental conditions.

Table 1. Height of taps to measure pressure and models of the transducers.

ti	Height, H (m)	Series/range
1*	0*	600/0-5psi
2	0.2620	600/0-1psi
3	0.3420	600/0-1psi
4	0.4420	600/0-1psi
5	1.080	860/0-1psi
6	1.580	860/0-1psi
7	2.580	860/0-1psi
8	2.880	860/0-1psi
9	3.180	860/0-1psi
10	3.430	860/0-1psi

*t1: Reference for all different H.

Table 2. Means and confidence intervals (95%) for all experimental conditions. The maximum capacity of the blower in the system was 38 m/s (nominal).

	Velocity (superficial)		Air flow rate	Temp.		Velocity (superficial)		Air flow rate	Temp.
	Set-v_n (m/s)	Mean (m/s)	m^3/h	˚C		Set-v_n (m/s)	Mean (m/s)	m^3/h	˚C
Only air	**14.0**	14.2 ± 0.2	113.8 ± 1.6	71.2 ± 1.4	Two-phase	**14.0**	14.4 ± 0.3	114.9 ± 2.1	70.5 ± 2.2
	22.0	22.2 ± 0.2	177.9 ± 1.9	52.0 ± 1.1		**22.0**	22.1 ± 0.1	176.0 ± 0.8	54.9 ± 0.8
	29.5	29.4 ± 0.3	235.2 ± 2.0	55.5 ± 0.9		**29.5**	29.5 ± 0.1	235.9 ± 0.3	59.5 ± 1.1
	38.0	38.2 ± 0.4	305.4 ± 3.2	61.3 ± 3.2		**38.0**	37.0 ± 0.2	295.9 ± 0.9	66.1 ± 1.4

2.2. Data Acquisition and Analysis

Software based on LabView 7.1 Express (National Instruments) managed the pressure data acquisition, using a cDAQ-9172 chassis (National Instruments) with the NI 9205 module (32-channel, +/−10 V, 250 kS/s, 16-bit analog input). Pressure time series data were collected at the same rate for each transducer signal. Different sampling frequencies were used in the trials, but all were at least 1000 Hz.

In each trial, average pressure values for each transducer were used to calculate the pressure drop with respect to t1 (reference for pressure drop equal to zero, at the zero mark height, H = 0). The same position was used as a reference to calculate the pressure drop in the simulations. The pressure drops measured in many trials were used to calculate the mean and standard deviation of the pressure drop at each height, together with the confidence interval (Student's t-distribution).

In both single- and two-phase flow, the pressure is expected to vary linearly along the height of the riser, for a region far away from the feeding section (entrance). For this reason, a linear model analysis was performed based on the coefficient of determination (R^2), in order to define the linear region.

2.3. Computational Domain and Mesh

Meshes (3D) were generated in Gambit 2.3 and the simulations were performed in Fluent 6.3. The reference was in the end of the feeding device and beginning of the riser (Z = 0).

The mesh building was based on a specific refinement of the mesh in the volume called the junction region, as shown in **Figure 2**, which indicates the computational domain near the feeding pipe. This region is the junction of the feeding pipe (conical) and the nozzle (cylindrical), resulting in a complex geometry. For this reason, the mesh there was tetrahedral, while hexahedral cells were used in the rest of the system.

A riser followed the exit of the venturi feeding device, and it was preceded by a straight pipe for air feeding. After the mesh in the junction region was built, the mesh in the feeding device was generated by making hexahedral cells with aspect ratios as close to 1:1 as possible. Subsequently, nodes in the axial direction were

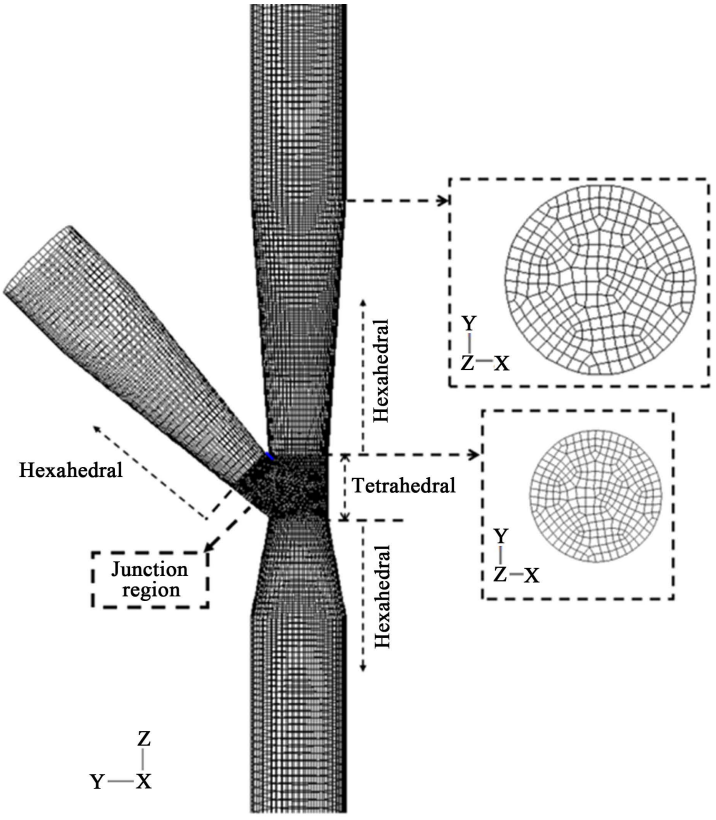

Figure 2. Mesh near the feeding device.

spaced in the riser and air entrance section, making the mesh coarser with distance from the feeding device. Consequently, the coarser cells were near the extremities of the riser (boundaries at the air entrance and the riser exit). For this reason, the specification of the mesh edges in the junction region provided sufficient information to obtain a close representation of the mesh in the whole system.

Simulations were performed with various mesh refinements (**Table 3**), each based on a different refinement at the junction region. A shorter riser was used in finer mesh simulations in order to reduce the computational time. Only the coarser mesh simulation used the same riser height as the experimental apparatus (**Figure 1**). Tests of solution stability showed that the mesh configuration was appropriate.

2.4. Multiphase Flow Model and Numerical Methods

The Eulerian granular kinetic theory model was employed for the solid phase modeling. The velocity (homogeneous) was used to define the inlet boundary condition, and zero relative pressure was assumed as the outlet boundary condition. The solids volume fraction was 0.6 at the inlet.

Two different values (zero and 0.2) were used for the wall specularity coefficient, in order to evaluate the effect of this boundary condition [16].

Most complementary models assume fast dilution of the particulate phase after entry into the riser. Since a high degree of dilution was obtained in the present system, the k-ε model for the dispersed phase and drag in diluted systems was used [17]. The granular and bulk viscosities have been described by Gidaspow *et al*. [18] and Lun *et al*. [19] respectively.

Green-Gauss node-based discretization and the SIMPLE coupling scheme were used for numerical solution. A transient solution procedure with time interval of 0.0001 s was adopted, with implicity time discretization and second order approximation for momentum and kinetic energy.

There have been no studies concerning the development of this type of flow in its initial stages, and it was not expected that the simulation would accurately represent the real system during the start-up. However, the granular flow stabilized after a certain time of simulation. At least 4 s of flow were necessary in all simulations, so the solution obtained at 9 s was adopted for comparisons of the fluid dynamics and pressure behavior. The presented averages were obtained from 9 s to 15 s.

3. Results and Discussion

3.1. Experimental Analysis of Solids Mass Flow Rate

In this type of feeding configuration, the solids mass flow rate is dependent on the air flow rate (**Figure 3**). Costa *et al*. [14] analyzed the regime transition using different approaches (plots of pressure drop against superficial velocity, voidage measurements, and pressure fluctuations) for a feeding system in which the mass flow rate of solids was dependent on the air flow rate. The criteria used for regime transitions in systems that maintained the solids mass flow rate when the gas flow rate was decreased could also be used for the system investigated here.

The analysis of pressure fluctuations was used to set the dilution conditions, and a highly restricted discharge area was needed to ensure dilute flows for a wide range of air flow rates. The analysis performed in the present work was similar to that described by Costa *et al*. [14] in all trials. The slide valve was set at 3% open in order to ensure stable dilute flow operation at different air flow rates.

The solids mass flow rate increased when the air flow rate was increased. Analysis of the experimental data to obtain a correlation between the solids mass flow rate and the air superficial velocity resulted in $R^2 = 0.97$ for the linear fit (**Figure 3**).

Table 3. Mesh refinements (3D simulations).

Riser height (m)	Refinement at junction region (mm)	Total number of cells
3.75	2.0	228,077
2.60	1.5	405,945
0.80	1.2	485,443

*Nozzle as feeder.

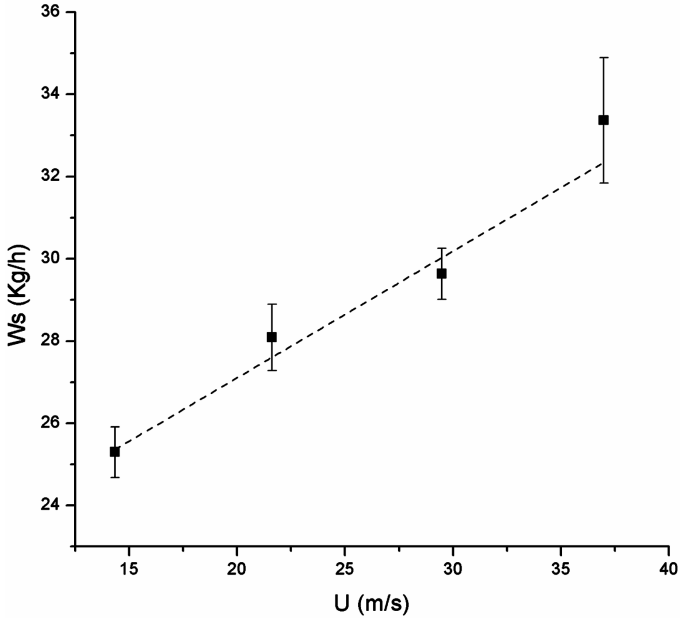

Figure 3. Solids flow rate according to air velocity. The bars represent 95% confidence intervals.

Costa *et al*. [14] used the Forchheimer equation to estimate the gas flow rate due to leakage on feeding, after measurement of the pressure drop in the feeding pipe. However, different to the previous findings, the impact of air leakage on feeding was considered irrelevant in the present case, because the pressure drop in the feeding pipe was less than 80 Pa/m. As a result, the lower pressure in the nozzle at higher air flow rates increased the solids discharge in the riser (**Figure 3**).

3.2. Experimental Pressure Data

Figure 4 shows the mean pressure drops obtained in all the trials, for single-and two-phase flows. Similar behavior was observed in both cases, with the local pressure drop increasing as the air flow rate increased, indicating the predominance of wall friction force over gravitational force, which is characteristic of dilute conveying.

A nominal velocity of 14 m/s was the velocity condition that resulted in greatest imprecision in the pressure data, since the values obtained were lower and adjustment of the air flow rate was less precise. For this reason, the lower air flow rate was not considered in the evaluation of the linear region. The linearity analysis for single-phase flow indicated that t4 up to t9 (notation in **Table 1**) corresponded to the linear pressure region, since the inclusion of t3 or t10 decreased the R^2 value for all conditions (with the exception of the lowest velocity).

All relevant information on the linear fitting for the data from t4 to t9 is presented in **Table 4**, including the R^2 values. Measurement was not made at t10 in the two-phase trials, because the purpose was to study only the riser and the single-phase measurements had already indicated that t10 was not in the linear region. The same linear region found for the single-phase data was also obtained for the two-phase dilute system, since the R^2 value decreased when data from t3 were included, except for the lower velocity.

The pressure drop in the linear pressure region increased when the superficial air velocity was increased, as expected for dilute conveying [14].

After defining the linear region, the slope obtained from the linear fitting of the pressure drop as a function of height could be used to estimate the pressure drop according to distance (**Table 4**) and characterize the pressure behavior in the region downstream of the feeding section.

Figure 5 shows the average pressure drops and the confidence intervals for the intermediate conditions. These data were used to evaluate the simulations.

It is important to note that the largest pressure drop was associated with the entrance of particles into the system, due to high momentum transfer between the phases in the feeding section.

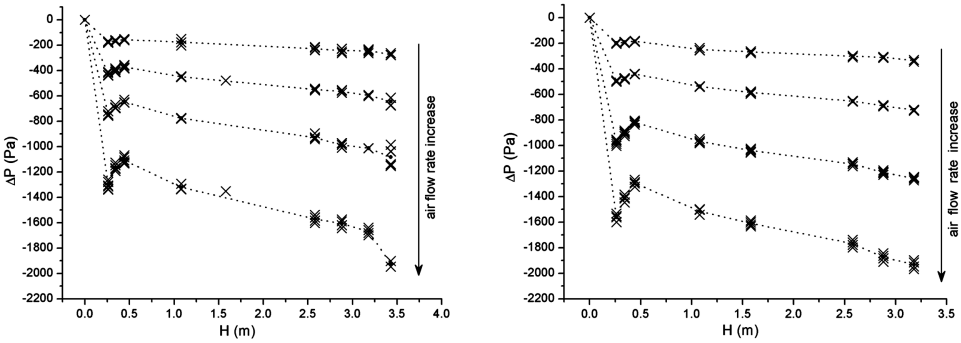

Figure 4. Mean pressure drop data for all trials: (a) Air flow; (b) Two-phase flow.

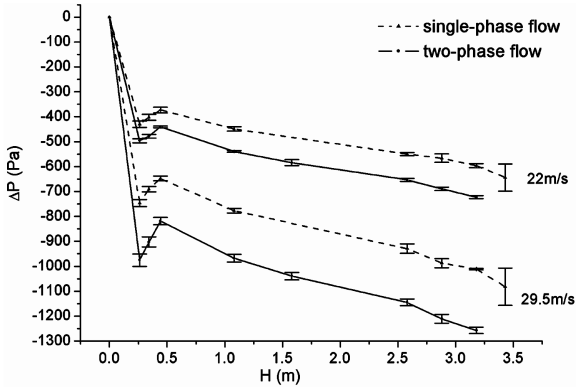

Figure 5. Plots of average pressure drop as a function of height in the riser. Error bars represent 95% confidence intervals.

Table 4. Linear analysis of the pressure drop using data from t4 to t9: Slope (ΔP/H), standard error (s), number of points used for linear fitting (n), and coefficient of determination (R^2).

	Single-phase				Two-phase			
v_n (m/s)	Δ P/H (Pa/m)*	s (Pa/m)	n	R^2	Δ P/H (Pa/m)*	s (Pa/m)	n	R^2
14	−33.8 ± 5.4	2.6	22	0.894	−48.0 ± 6.7	3.2	18	0.935
22	−78.7 ± 4.5	2.2	24	0.984	−95.4 ± 6.3	3.0	24	0.979
29.5	−131.0 ± 7.9	3.8	24	0.982	−149.4 ± 8.8	4.3	30	0.977
38	−199.8 ± 15.0	7.2	22	0.975	−220.2 ± 16.5	7.9	23	0.974

3.3. Simulation Conditions, Initial Analysis, and Pressure Verification

Intermediate conditions were used for simulation, avoiding the maximum capacity of the blower and the lowest air flow rate, for which there were greater uncertainties in the measurements. An air flow rate of 235.2 m^3/h (v_n = 29.5 m/s) was selected for simulation and detailed characterization. This condition resulted in a solids flow rate of 29.6 kg/h.

The phase volume fraction fields of the multiphase flow simulations supported the assumption of fast dilution, which was adopted in the modeling of this system, as can be seen in **Figure 6**. The solid phase fraction decreased from 0.6 to less than 0.01 as soon as the solids entered the conveying pipe.

Simulation using different specularity coefficients showed that this parameter affected the pressure profile through the riser, with the greatest differences occurring in the linear pressure region (**Figure 7**).

The pressure drops in the linear region predicted by the simulations were −181 Pa/m (specularity coefficient of zero) and −209 Pa/m (coefficient of 0.2). Both values overestimated the experimental data (−149.4 ± 8.8 Pa/m).

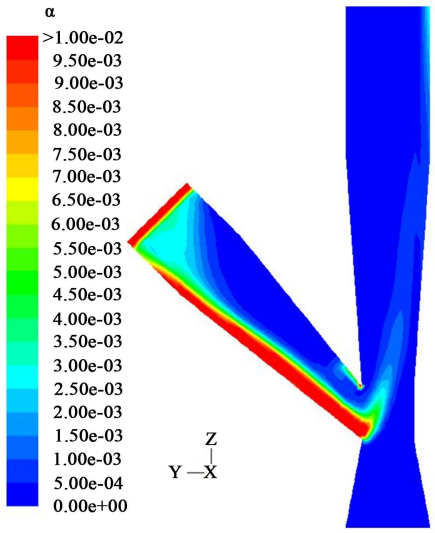

Figure 6. Solids volume fraction fields near the feeding section.

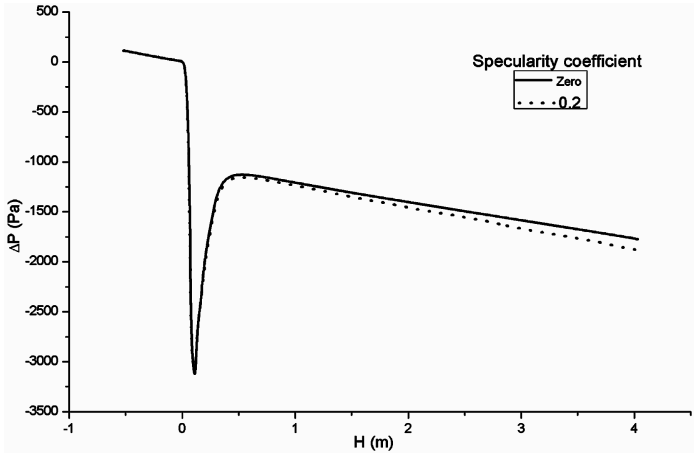

Figure 7. Average pressure drop along the axis of the computational domain for two different specularity coefficients and 2 mm mesh.

Since use of the smaller specularity coefficient resulted in the best representation of the experimental data, details concerning the fluid dynamics are only given for this condition.

The experimental data were compared with the simulated pressures for all the meshes used (**Figure 8**). Decrease of the mesh from 2 mm to 1.5 mm considerably improved the pressure prediction. However, further reduction of the mesh resulted in a slightly poorer fit to the experimental data.

The simulated pressures were quite close to the experimental data. Moreover, inclusion of the solid phase did not greatly increase the error of the simulation, compared to the single-phase flow simulation. **Figure 9** presents a comparison of the simulated and experimental pressure data for single-phase flow. In the air flow simulations, the pressure drop in the linear region was estimated to be −172 Pa/m (mesh based on 1.2 mm). It should be noted that the error in the pressure drop for the linear pressure region was around 30 - 40 Pa/m for the single- and two-phase flows.

3.4. Fluid Dynamics Using Eulerian Simulation

Despite the pressure difference observed when comparing the results for the 2 mm and 1.5 mm meshes, both simulations showed similar fluid dynamics for the solid phase. In the following discussion, comments concerning the similarity are included where appropriate, but the focus is mainly on the 1.5 mm mesh.

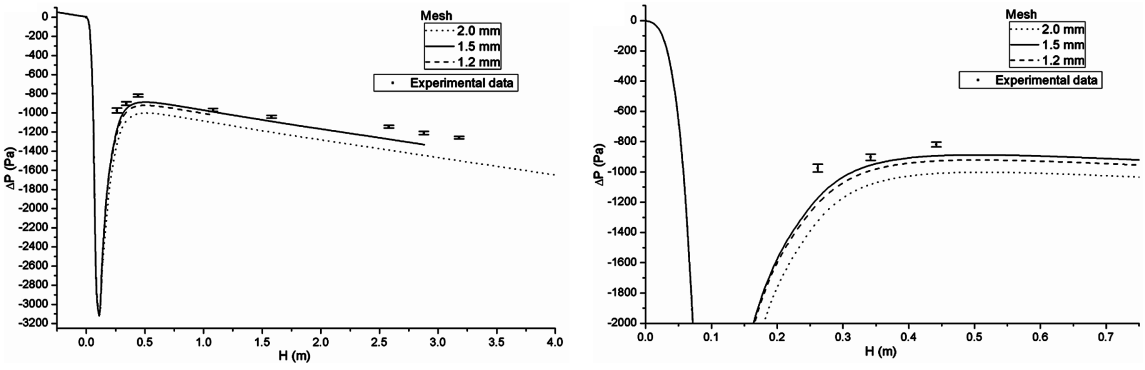

Figure 8. Average simulated pressure drop along the axis of the computational domain for the lower specularity coefficient, and comparison with experimental data.

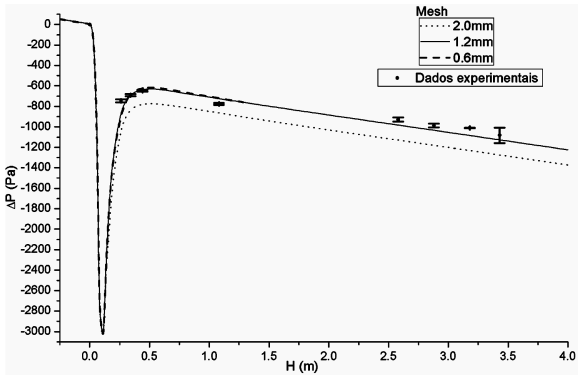

Figure 9. Average simulated pressure drop along the axis of the computational domain for single-phase flow, and comparison with experimental data.

For solids volume fractions higher than 0.0001, clusters were formed near the feeding device. The formation of one of these clusters is shown in **Figure 10**. The clusters were diluted, but the volume fractions present were sufficiently high to distinguish them from other areas of the multiphase flow. Cluster formation was also observed in the simulations with shorter riser and finer mesh.

The resolution of the fields was compromised due to the high dilution ratio in the system, and the procedure used to present the fields did not enable visualization of details for volume fractions higher than 10^{-4}. However, the fields are sufficiently clear to be able to distinguish the radial and axial behavior of the solids volume fraction.

Cluster formation occurred continuously in the riser, and larger cluster structures were usually found in the downstream section. **Figure 11** shows the tendency of cluster A (from **Figure 10**) to merge with another cluster (B, in **Figure 11**) formed previously in the system.

Clusters produced as described above were continuously seen in the end of the riser, which means that cluster formation at the feeder could influence the behavior throughout the riser. Analogous cluster propagation along the riser was observed for the longer system that was simulated using 2 mm mesh.

Similar behavior was obtained in simulations with specularity coefficient of 0.2. However, the formation of clusters was apparently more intense. Further studies will be needed in order to describe and quantify these effects with greater accuracy.

The solids showed a tendency to accumulate in the opposite side of the feeding pipe, due to the high specific mass and inertia of this phase. The accumulation region was revealed by the dynamic behavior, as can be seen in the average field (**Figure 12**).

However, the presence of the clusters had the effect of spreading the average solid phase volume fraction during the advance through the riser (**Figure 13**). The solid phase volume fraction was relatively homogeneous in the radial direction for sections closer to the riser exit, despite a slightly higher concentration near the wall.

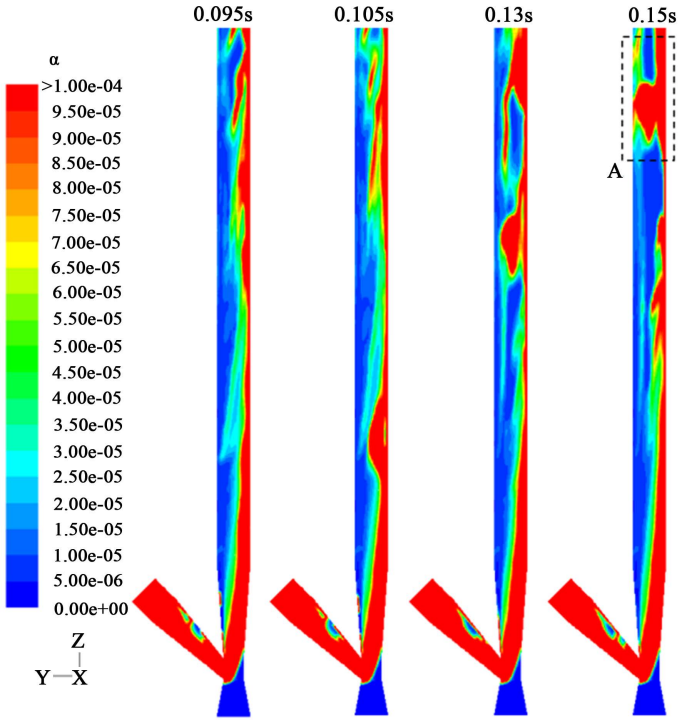

Figure 10. Dynamic behavior of the two-phase flow near the feeding device (0.87 m of riser). The dashed region with letter A highlights a cluster.

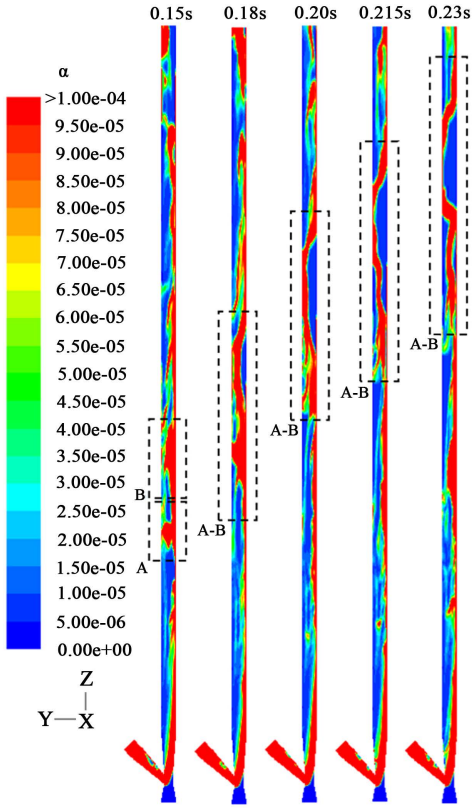

Figure 11. Dynamic behavior of the two-phase flow from the feeding device to a riser height of 2.6 m.

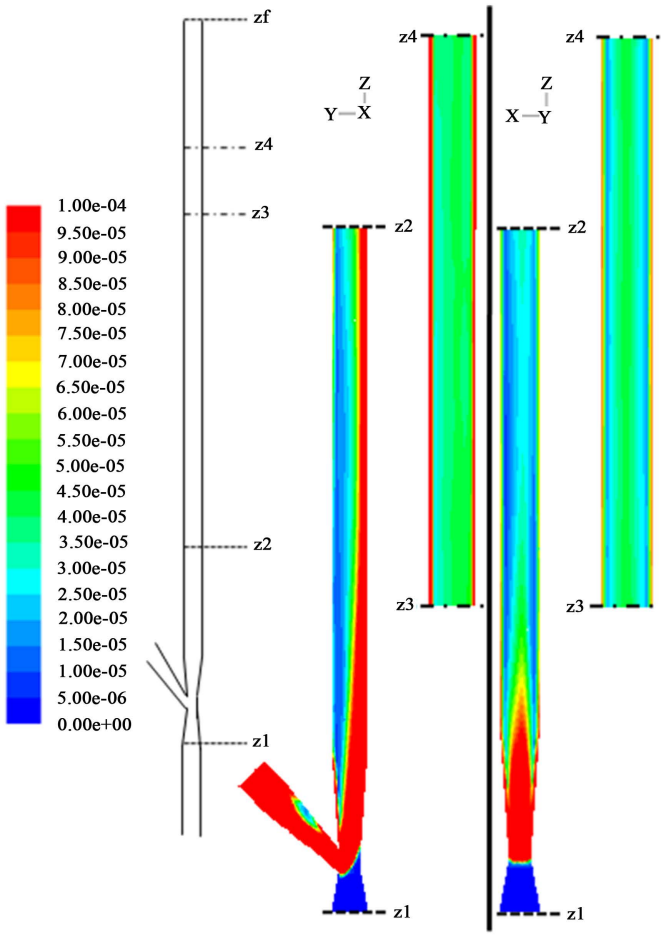

Figure 12. Average solids volume fraction field. z3 = 2.82 m and z4 = 3.50 m (2.0 mm mesh); z1 = −0.235 m and z2 = 0.72 m (1.5 mm mesh).

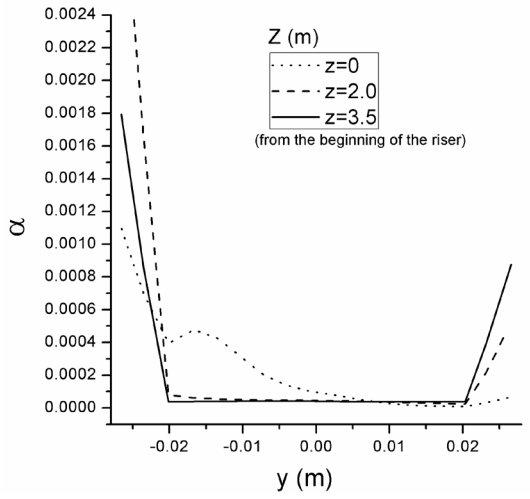

Figure 13. Average solids volume fraction field.

4. Conclusions

The experimental solids flow rate presented a linear relationship with the air flow rate for the vertical venturi

feeder, due to the decreasing pressure in the throat and no appreciable leakage through the feeding pipe. The experimental assays revealed a relatively low mass flow rate in the conveyor, emphasizing the importance of scaling up this system for application at an industrial scale. Scale-up could be assisted by the development of a reliable CFD model for this type of equipment.

The specularity coefficient affected the pressure drop, with the greatest effect seen in the linear region. The formation of clusters was apparently more intense for the higher specularity coefficient. Further studies will be needed in order to describe and quantify these effects with greater accuracy. For the experimental data acquired in this work, the closest estimation of pressure drop was achieved using a specularity coefficient of zero, and this value was used to describe the detailed fluid dynamics of the solid phase.

There have only been a modest number of studies reported in the literature concerning the feeding of coarse particles directly into a riser. The present work therefore contributes to providing information about such systems, with the aid of simulations. Evaluation of the fluid dynamics and average fields showed that the solids tended to accumulate near the wall in the feeding section. The simulated fluid dynamics of the solid phase showed the formation of clusters in the feeding section. These clusters usually continued throughout the riser, with periodic assembly of other clusters.

Simulations showed that clusters frequently endured until the end of the riser, indicating that perturbation of the coarse particulate phase in the feeding section of the riser was more significant than observed previously for fine particles conveyed in a riser with similar diameter (FCC catalyst) [20].

Accumulation near the wall, especially close to the feeding section, and clusters indicate a potential risk of agglomeration of material, heterogeneous heating and drying. These findings emphasize the importance of selection of a suitable feeding device in pneumatic conveying dryers. CFD simulations can be used to analyze behavior in the riser and to evaluate methods of improving the gas-solid mixture. However, it would be important to determine the relative importance of the fluid dynamics and heating during the drying process. Simulation with non-cohesive particles is a step towards CFD simulations that include the drying process and cohesive phenomena (agglomeration). The principal remaining obstacle to comprehensive simulation is the inclusion of particle agglomeration.

Acknowledgements

The authors thank CAPES (Coordenação de Aperfeiçoamento de Pessoal de Nível Superior) and CNPq (Conselho Nacional de Desenvolvimento Científico e Tecnológico) for financial support.

References

[1] Hidayat, M. and Rasmuson, A. (2004) Numerical Assessment of Gas-Solid Flow in a U-Bend. Chem. *Research in Engineering Design*, **82**, 332-343. http://dx.doi.org/10.1205/026387604322870444

[2] Hidayat, M. and Rasmuson, A. (2007) Heat and Mass Transfer in U-Bend of a Pneumatic Conveying Dryer. *Chemical Engineering Research and Design*, **85**, 307-319. http://dx.doi.org/10.1205/cherd06162

[3] Rajan, K.S., Dhasandhan, K., Srivastava, S.N. and Pitchumani B. (2008) Studies on Gas-Solid Heat Transfer during Pneumatic Conveying. *International Journal of Heat and Mass Transfer*, **51**, 2801-2813. http://dx.doi.org/10.1016/j.ijheatmasstransfer.2007.09.042

[4] Sousa, R.C., Almeida, A.R.F., Ferreira, M.C. and Freire, J.T. (2010) Analysis of Fluid Dynamics and Thermal Behavior Using a Vertical Conveyor with a Spouted Bed Feeder. *Drying Technology*, **28**, 1277-1287. http://dx.doi.org/10.1080/07373937.2010.483031

[5] Fokeer, S., Kingman, S., Lowndes, I. and Reynolds, A. (2004) Characterisation of the Cross Sectional Particle Concentration Distribution in Horizontal Dilute Flow Conveying—A Review. *Chemical Engineering and Processing*, **43**, 677-691. http://dx.doi.org/10.1016/S0255-2701(03)00096-5

[6] Zhu, K.W., Rao, S.M., Wang, C.H. and Sundaresan, S. (2003) Electrical Capacitance Tomography Measurements on Vertical and Inclined Pneumatic Conveying of Granular Solids. *Chemical Engineering Science*, **58**, 4225-4245. http://dx.doi.org/10.1016/S0009-2509(03)00306-3

[7] Vashisth, S. and Grace, J.R. (2012) Simulation of Granular Transport of Geldart Type-A, -B, and -D Particles through a 90 Degrees Elbow. *Industrial & Engineering Chemistry Research*, **51**, 2030-2047. http://dx.doi.org/10.1021/ie200647e

[8] Grbavcic, Z.B., Garic, R.V., Jovanovic, S.D. and Rozic, L.S. (1997) Hydrodynamic Modeling of Vertical Accelerating

Gas-Solid Flow. *Powder Technology*, **92**, 155-161. http://dx.doi.org/10.1016/S0032-5910(97)03234-8

[9] Lopes, C.S., Pádua, T.F., Ferreira, M.C. and Freire, J.T. (2011) Influence of the Entrance Configuration on the Performance of a Non-Mechanical Solid Feeding Device for a Pneumatic Dryer. *Drying Technology*, **29**, 1186-1194. http://dx.doi.org/10.1080/07373937.2011.575495

[10] Rajan, K.S., Srivastava, S.N., Pitchumani, B. and Mohanty, B. (2006) Simulation of Gas-Solid Heat Transfer during Pneumatic Conveying: Use of Multiple Gas Inlets along the Duct. *International Communications in Heat and Mass Transfer*, **33**, 1234-1242. http://dx.doi.org/10.1016/j.icheatmasstransfer.2006.06.011

[11] Grace, J.R. and Taghipour, F. (2004) Verification and Validation of CFD Models and Dynamic Similarity for Fluidized Beds. *Powder Technology*, **139**, 99-110. http://dx.doi.org/10.1016/j.powtec.2003.10.006

[12] Du, B., Warsito, W. and Fan, L.S. (2004) ECT Studies of the Choking Phenomenon in a Gas-Solid Circulating Fluidized Bed. *AIChE Journal*, **50**, 1386-1406. http://dx.doi.org/10.1002/aic.10168

[13] Chan, C.W., Seville, J.P.K., Parker, D.J. and Baeyens, J. (2010) Particle Velocities and Their Residence Time Distribution in the Riser of a CFB. *Powder Technology*, **203**, 187-197. http://dx.doi.org/10.1016/j.powtec.2010.05.008

[14] Costa, I.A., Ferreira, M.D. and Freire, J.T. (2004) Analysis of Regime Transitions and Flow Instabilities in Vertical Conveying of Coarse Particles Using Different Solids Feeding Systems. *The Canadian Journal of Chemical Engineering*, **82**, 48-59. http://dx.doi.org/10.1002/cjce.5450820107

[15] Mills, D. (2004) Pneumatic Conveying Design Guide. Elsevier Butterworth-Heinemann, Oxford.

[16] Béttega, R., Rosa, C.A., Corrêa, R.G. and Freire, J.T. (2009) Fluid Dynamic Study of a Semicylindrical Spouted Bed: Evaluation of the Shear Stress Effects in the Flat Wall Region Using Computational Fluid Dynamics. *Industrial & Engineering Chemistry Research*, **48**, 11181-11188. http://dx.doi.org/10.1021/ie900973x

[17] Wen, C.Y. and Yu, Y.H. (1966) Mechanics of Fluidization. *The Chemical Engineering Progress Symposium Series*, **162**, 100-111.

[18] Gidaspow, D., Bezburuah, R. and Ding J. (1992) Hydrodynamics of Circulating Fluidized Beds, Kinetic Theory Approach. In: Potter, O.E. and Nicklin, D.J., Eds., Fluidization VII, *Proceedings of the* 7*th Engineering Foundation Conference on Fluidization*, Engineering Foundation, New York, 75-82.

[19] Lun, C.K.K., Savage, S.B., Jeffrey, D.J. and Chepurniy, N. (1984) Kinetics Theories for Granular Flow: Inelastic Particles in Couette Flow and Slightly Inelastic Particles in a General Flowfield. *Journal of Fluid Mechanics*, **140**, 223-256. http://dx.doi.org/10.1017/S0022112084000586

[20] Wilde, de J., Van Engelandt, G., Heyndenickx, G.J. and Marin, G.B. (2005) Gas Solids Mixing in the Inlet Zone of a Dilute Circulating Fluidized Bed. *Powder Technology*, **151**, 96-116. http://dx.doi.org/10.1016/j.powtec.2004.11.037

Nomenclature

H—Height in the riser (flow length) [m]
r—Radial direction [m]
t_i—Tap number [m/s]
Ug—Gas phase superficial velocity [m/s]
v_n—Nominal velocity [m/s]
Ws—Solid phase flow rate [Kg/h]
Greek Letters
α—Phase volume fraction
ΔP—Pressure drop [Pa]
Subscripts
s—Solid
g—Gas